

EXTENDED KALMAN FILTER BASED STATES ESTIMATION OF UNMANNED QUADROTORS FOR ALTITUDE-ATTITUDE TRACKING CONTROL

Mouna GHANAI, Ali MEDJGHOU, Kheireddine CHAFAA

LAAAS, Electronics Department, Faculty of Technology, University of Batna 2,
Constantine road 53, Fesdis, 05078 Batna, Algeria

m.ghanai@univ-batna2.dz, a.medjghou@univ-batna2.dz, k.chafaa@univ-batna2.dz

DOI: 10.15598/aeec.v16i4.2911

Abstract. In this paper, state variables estimation and Fuzzy Sliding Mode Control (FSMC) are presented in order to estimate the state variables and altitude-attitude tracking control in presence of internal and external disturbances for unmanned quadrotor. The main idea of the proposed control strategy is the development of an Extended Kalman Filter (EKF) for the observation of the states. Fuzzy logic systems are used to adapt the unknown switching-gains to eliminate the chattering phenomenon induced by Sliding Mode Control (SMC). The stability of the system is guaranteed in the sense of Lyapunov. The effectiveness and robustness of the proposed controller-observer scheme that takes into account internal and external disturbances are demonstrated on computer simulation using Matlab environment.

Keywords

Altitude and attitude tracking, extended Kalman filter, fuzzy sliding mode control, quadrotor.

1. Introduction

In recent years, Unmanned Aerial Vehicles (UAVs) have become a topic of interest in many research organizations due to their wide applications in several areas, such as enforcement of traffic rules and road networks surveillance, industrial plants and high-tension power lines, mapping three-dimensional environments. A quadrotor is a typically under-actuated because it has six degrees of freedom and only four actual inputs, and it is a nonlinear coupled system due to the aerodynamics of its four rotors. Moreover, during the flight

in low attitude, it is susceptible, which influences the flight performance or even leads to instability [1] and [2]. However, the difficulty of a controller design increases due to these constraints. Altitude and attitude tracking control are of main interests in quadrotors study. It has attracted much attention from researchers due to its potential practical applications [3]. The attitude controller is an important feature since it allows the vehicle to maintain a desired orientation and hence prevents the vehicle from flipping over and crashing [4].

In the literature, several control algorithms have been proposed to altitude and attitude control of unmanned quadrotor systems such as backstepping based controller [5], fuzzy logic based controller, and sliding mode controller [6] and [7]. Sliding control is well known for its effectiveness through the theoretical studies versus the parameter variations and disturbances, and has been widely applied to robotics and aircraft control design. Chattering phenomenon (high frequency of control action) is the major problem associated with SMC, which is caused by the inappropriate selection of the switching gain. In order to reduce the chattering phenomenon, various methods have been proposed in the literature [7] and [8].

In practice, the state variables of a given system are rarely available for direct measurement. The elaboration of a control law for this system often requires access to the value of one or more of its states. For this reason, it is necessary to design an auxiliary dynamic system named observer, capable to deliver state estimates from the measurements provided by physical sensors and applied inputs. In the case of nonlinear systems, there is not a general solution to the problem of observer synthesis, which prompted researchers to develop nonlinear observers such as sliding mode observer [9], High order sliding mode observer [10], Ex-

tended Kalman filter [11], fuzzy logic observer [12], and artificial neural network observer [13].

EKF is an optimal recursive estimator, which can be used for estimating the state of nonlinear systems [14]. In the last decade, EKF was widely used for stochastic nonlinear systems. EKF provides the suboptimal state estimator for its ability to consider the stochastic uncertainties, which is the case of quadrotor UAVs. EKF is a recursive algorithm, and it is known for its high convergence rate, which improves transient performance significantly. Compared to other nonlinear observers [15], [16], [17], [18] and [19], EKF algorithm has better dynamic behavior, resistance to uncertainties and noise, and it can work even in the presence of a standstill conditions.

In [20], the authors presented stabilizing control laws synthesis using sliding mode technique, and used the EKF to estimate the unmeasured states. The controlled model was very simple because the authors did not consider the nonlinearities, uncertainties, external perturbations, and nonholonomic constraints.

In [21], the authors presented a state estimation of the quadrotor UAV based on a high degree cubature Kalman filter, but they did not illustrate the design method of the controller and stability analysis of closed-loop system.

In [22], a Radical Basis Function Neural Networks (RBFNNs) and double-loop integral sliding mode control are presented for the position and attitude tracking of quadrotor subjected to parameter uncertainties and sustained disturbances. In [23], a novel adaptive fuzzy gain-scheduling sliding mode control is studied for attitude regulation of an unmanned quadrotors with parametric uncertainties and external disturbances. In [24], the authors explored the design of an SMC for trajectory tracking for an unmanned aerial vehicle. Note that in both of last two cited works, the influences of the nonholonomic constraints and the observation problem were not discussed. Moreover, in [25], the authors designed a fuzzy sliding mode control based on backstepping synthesis for unmanned quadrotors, in which the observation problem was not considered.

In this investigation, two major contributions are proposed:

- An EKF for estimating the state space vector.
- A robust altitude-attitude Fuzzy Sliding Mode Controller (FSMC) in the presence of both internal and external disturbances.

In order to reduce chattering phenomenon, a Fuzzy Logic System (FLS) is designed to adapt the unknown switching-gains by fuzzifying the sliding surface according to the fuzzy inference rule base. Lyapunov synthesis is used to determine the stability analysis of the

closed-loop system. Performances of the controller-observer are illustrated by a simulation study that takes into account internal disturbances including the Gaussian white noise process and measurement noise, and external disturbances.

The presented paper is organized as follows. In Sec. 2, dynamic modeling of a quadrotor is introduced. In Sec. 3, state space representation and discretization of the quadrotor model are formulated, whereas in Sec. 4, we recall the basic mathematical formulas of the EKF. Section 5 is dedicated to the proposed controller-observer design and closed loop stability. In Sec. 6, we present simulation studies that illustrate the performance of the proposed controller-observer system. Finally, conclusions are summarized in Sec. 7.

2. Quadrotor Dynamic Modelling

The quadrotor adopted in this investigation was introduced in [1] and [2] (see Fig. 1).

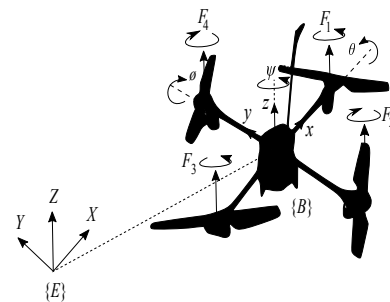


Fig. 1: Quadrotor configuration [1] and [2].

Using the Newton-Euler laws of mechanics, the motion equations of the quadrotor can be written as follows:

$$\begin{cases} \ddot{\phi} = 1/I_x \{ \dot{\theta} \dot{\psi} (I_y - I_z) - K_{f_{ax}} \dot{\phi}^2 - J_r \bar{\Omega} \dot{\theta} + l u_2 + d \}, \\ \ddot{\theta} = 1/I_y \{ \dot{\phi} \dot{\psi} (I_z - I_x) - K_{f_{ay}} \dot{\theta}^2 + J_r \bar{\Omega} \dot{\phi} + l u_3 + d \}, \\ \ddot{\psi} = 1/I_z \{ \dot{\theta} \dot{\phi} (I_x - I_y) - K_{f_{az}} \dot{\psi}^2 + u_4 + d \}, \\ \ddot{x} = 1/m \{ u_x u_1 - K_{f_{tx}} \dot{x} + d \}, \\ \ddot{y} = 1/m \{ u_y u_1 - K_{f_{ty}} \dot{y} + d \}, \\ \ddot{z} = 1/m \{ (\cos \phi \cos \theta) u_1 - K_{f_{tz}} \dot{z} \} - g_a + d, \end{cases} \quad (1)$$

where m is the total mass of the quadrotor, d represents the disturbances applied to the quadrotor, l is the distance between the mass centre of the quadrotor and the rotation axis of propeller, and $\bar{\Omega} = (\omega_1 - \omega_2 + \omega_3 - \omega_4)$ is the total gyroscopic torques which affect the quadrotor. $K_{fa} = \text{diag}(K_{f_{ax}}, K_{f_{ay}}, K_{f_{az}})$ represents the aerodynamics frictions factors. J_r is the total rotational moment of inertia around the propeller axis.

Finally, u_x and u_y are two virtual control inputs:

$$\begin{cases} u_x = \cos \phi \sin \theta \cos \psi + \sin \phi \sin \psi, \\ u_y = \cos \phi \sin \theta \sin \psi - \sin \phi \cos \psi. \end{cases} \quad (2)$$

From Eq. (2), it is easy to show that :

$$\begin{cases} \phi_d = \arcsin [u_x \sin(\psi_d) - u_y \cos(\psi_d)], \\ \theta_d = \arcsin \left[\frac{u_x \cos(\psi_d) + u_y \sin(\psi_d)}{\cos(\phi_d)} \right]. \end{cases} \quad (3)$$

3. State Space Representation

Let $X = (\phi, \dot{\phi}, \theta, \dot{\theta}, \psi, \dot{\psi}, x, \dot{x}, y, \dot{y}, z, \dot{z})^T \in \mathbb{R}^{12}$, $u = (u_1, u_2, u_3, u_4)^T \in \mathbb{R}^4$ and $Y = (x_1, x_3, x_5, x_7, x_9, x_{11})^T$ be the state, the control input and the output vectors, respectively.

The dynamic model given in Eq. (1) can be written using the state space method as:

$$\begin{cases} \dot{x}_1 = x_2, \\ \dot{x}_2 = f_1(X) + g_1(X)u_2 + d, \\ \dot{x}_3 = x_4, \\ \dot{x}_4 = f_2(X) + g_2(X)u_3 + d, \\ \dot{x}_5 = x_6, \\ \dot{x}_6 = f_3(X) + g_3(X)u_4 + d, \\ \dot{x}_7 = x_8, \\ \dot{x}_8 = f_4(X) + g_4(X)u_1 + d, \\ \dot{x}_9 = x_{10}, \\ \dot{x}_{10} = f_5(X) + g_5(X)u_1 + d, \\ \dot{x}_{11} = x_{12}, \\ \dot{x}_{12} = f_6(X) + g_6(X)u_1 + d, \end{cases} \quad (4)$$

where

$$\begin{aligned} f_1(X) &= [a_1 x_4 x_6 + a_2 x_2^2 + a_3 \bar{\Omega} x_4], f_4(X) = [a_9 x_8], \\ f_2(X) &= [a_4 x_2 x_6 + a_5 x_4^2 + a_6 \bar{\Omega} x_2], f_5(X) = [a_{10} x_{10}], \\ f_3(X) &= [a_7 x_2 x_4 + a_8 x_6], \\ f_6(X) &= [a_{11} x_{12} - g_a], \\ g_1(X) &= b_1, g_2(X) = b_2, g_3(X) = b_3, g_4(X) = \frac{u_x}{m}, \\ g_5(X) &= \frac{u_y}{m}, g_6(X) = \frac{\cos x_1 \cos x_3}{m}, \end{aligned}$$

in which:

$$\begin{aligned} a_1 &= (I_y - I_z)/I_x, & a_2 &= -K_{f_{ax}}/I_x, \\ a_3 &= -J_r/I_x, & a_4 &= (I_z - I_x)/I_y, \\ a_5 &= -K_{f_{ay}}/I_y, & a_6 &= J_r/I_y, \\ a_7 &= (I_x - I_y)/I_z, & a_8 &= -K_{f_{az}}/I_z, \\ a_9 &= -K_{f_{tx}}/m, & a_{10} &= -K_{f_{ty}}/m, \\ a_{11} &= -K_{f_{tz}}/m, & b_1 &= l/I_x, b_2 = l/I_y, b_3 = 1/I_z. \end{aligned}$$

Since the Kalman filter is a discrete algorithm, discretization of the model is needed. The resulting global discrete form will be given by the following discrete nonlinear representation:

$$\begin{cases} x_1(k+1) = x_1(k) + \Delta t x_2(k) + w_1(k), \\ x_2(k+1) = x_2(k) + \Delta t f_{11} + w_2(k), \\ x_3(k+1) = x_3(k) + \Delta t x_4(k) + w_3(k), \\ x_4(k+1) = x_4(k) + \Delta t f_{22} + w_4(k), \\ x_5(k+1) = x_5(k) + \Delta t x_6(k) + w_5(k), \\ x_6(k+1) = x_6(k) + \Delta t f_{33} + w_6(k), \\ x_7(k+1) = x_7(k) + \Delta t x_8(k) + w_7(k), \\ x_8(k+1) = x_8(k) + \Delta t f_{44} + w_8(k), \\ x_9(k+1) = x_9(k) + \Delta t x_{10}(k) + w_9(k), \\ x_{10}(k+1) = x_{10}(k) + \Delta t f_{55} + w_{10}(k), \\ x_{11}(k+1) = x_{11}(k) + \Delta t x_{12}(k) + w_{11}(k), \\ x_{12}(k+1) = x_{12}(k) + \Delta t f_{66} + w_{12}(k), \end{cases} \quad (5)$$

where $f_{11} = [f_1(X) + g_1(X)u_2(k) + d_k]$, $f_{22} = [f_2(X) + g_2(X)u_3(k) + d_k]$, $f_{33} = [f_3(X) + g_3(X)u_4(k) + d_k]$, $f_{44} = [f_4(X) + g_4(X)u_1(k) + d_k]$, $f_{55} = [f_5(X) + g_5(X)u_1(k) + d_k]$, $f_{66} = [f_6(X) + g_6(X)u_1(k) + d_k]$,

$$h = Z = \begin{cases} x_1(k) + v_1(k), \\ x_3(k) + v_2(k), \\ x_5(k) + v_3(k), \\ x_7(k) + v_4(k), \\ x_9(k) + v_5(k), \\ x_{11}(k) + v_6(k). \end{cases} \quad (6)$$

Δt is the sampling period and $k \in \mathbb{Z}$ is the discrete-time points.

4. Extended Kalman Filter

The Kalman filter was developed by R. E. Kalman in 1960 [26]. EKF is a generalization of the Kalman filter which is a stochastic observer for nonlinear dynamical systems. In this paper, we shall attempt to find the best estimate of the state vector X_k of the system, which evolves according to the following discrete-time nonlinear dynamic:

$$\begin{cases} X_{k+1} = f(X_k, u_k, w_k), \\ Z_k = h(X_k, v_k), \end{cases} \quad (7)$$

where $f(\cdot)$ represents the evolution function of the system, $h(\cdot)$ represents the relationship between the state vector and the measurement result Z_k , whereas u_k stands for the control input to the system at step k , and w_k and v_k are the process and measurement white Gaussian noise vectors with zero mean and with associated covariance matrices $Q = E[w_k, w_k]^T$ and $R = E[v_k, v_k]^T$, respectively.

To apply EKF to the nonlinearity given in Eq. (7), it must be linearized by using the first order Taylor approximation around the desired reference point $(\hat{X}_k, \hat{w}_k = 0, \hat{v}_k = 0)$, which gives us the following

approximated linear model:

$$\begin{cases} X_{k+1} \approx f(X_k, u_k, w_k) \approx \\ \approx f(\hat{X}_k, u_k, 0) + F_k(X_k - \hat{X}_k) + W_k(w_k - 0), \\ Z_k \approx h(X_k, v_k) \approx \\ \approx h(\hat{X}_k, 0) + H_k(X_k - \hat{X}_k) + V_k(v_k - 0), \end{cases} \quad (8)$$

where the Jacobean matrices of f and h are given as follows:

$$F_k = \left. \frac{\partial f(X,0)}{\partial X} \right|_{X=\hat{X}}, \quad W_k = \left. \frac{\partial f(\hat{X}_k,w)}{\partial w} \right|_{w=0},$$

$$H_k = \left. \frac{\partial h(X,0)}{\partial X} \right|_{X=\hat{X}} \quad \text{and} \quad V_k = \left. \frac{\partial h(\hat{X}_k,v)}{\partial v} \right|_{v=0}.$$

The EKF is a recursive algorithm that is used for estimating state vector. It can be given by the following recursive equations:

Prediction:

$$\begin{aligned} \hat{X}_{k+1/k} &= f(\hat{X}_{k/k}, u_k, 0), \\ P_{k+1/k} &= F_k P_{k/k} F_k^T + W_k Q W_k^T, \end{aligned} \quad (9)$$

Correction:

$$\begin{aligned} \hat{X}_{k+1/k+1} &= \hat{X}_{k+1/k} + K_k(Z_k - h(\hat{X}_{k+1/k}, 0)), \\ P_{k+1/k+1} &= P_{k+1/k} - K_k H_k P_{k+1/k}, \end{aligned} \quad (10)$$

Kalman filter gain matrix:

$$K_k = P_{k+1/k} H_k^T (H_k P_{k+1/k} H_k^T + V_k R V_k^T)^{-1}, \quad (11)$$

where $\hat{X}_{k+1/k+1}$ denotes the posteriori state prediction vector, $\hat{X}_{k+1/k}$ is the priori state prediction vector, $P_{k+1/k+1}$ denotes the posteriori prediction error covariance matrix, and $P_{k+1/k}$ is the priori prediction error covariance matrix.

EKF framework is presented in Fig. 2.

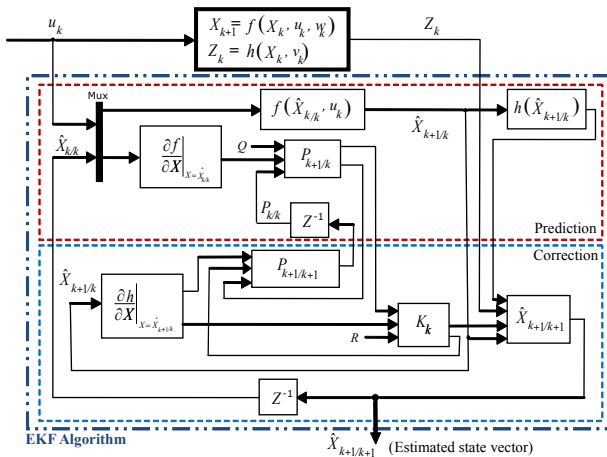


Fig. 2: Extended Kalman filter framework.

5. Controller Design and Stability Analysis

For the development of the control laws, the following assumptions are needed:

Assumption 1. The pitch, roll, and yaw angles satisfy the following inequalities: $-\pi/2 \leq \phi(t) \leq \pi/2$, $-\pi/2 \leq \theta(t) \leq \pi/2$ and $-\pi \leq \psi(t) \leq \pi$.

Assumption 2. The function f is assumed to be known and the error on its estimate is bounded, i.e. $|f(\hat{X}) - f(X)| \leq M$, where \hat{X} is an estimate have used an EKohave used an EKF X , and $M < 0$.

Assumption 3. The input gain g is assumed to be known and bounded, i.e. $0 < g_{\min} \leq g(X) \leq g_{\max}$.

Assumption 4. The disturbances d in the discrete dynamic model are unknown but bounded, i.e. $|d| \leq D$, where $D \geq 0$.

Assumption 5. The desired trajectory X_d and its first and second time derivatives are available and assumed to be bounded.

The objective is to estimate the velocity $\{x_2, x_4, x_6, x_8, x_{10}, x_{12}\} = \{\dot{\phi}, \dot{\theta}, \dot{\psi}, \dot{x}, \dot{y}, \dot{z}\}$, and to design a robust tracking controller so that the state vector $X = \{x_1, x_2, \dots, x_{12}\}^T = \{\phi, \dot{\phi}, \theta, \dot{\theta}, \psi, \dot{\psi}, x, \dot{x}, y, \dot{y}, z, \dot{z}\}^T$ can track a given desired reference $X_d = \{x_{d1}, x_{d2}, \dots, x_{d12}\} = \{\phi_d, \dot{\phi}_d, \theta_d, \dot{\theta}_d, \psi_d, \dot{\psi}_d, x_d, \dot{x}_d, y_d, \dot{y}_d, z_d, \dot{z}_d\}^T$ in finite-time, even in presence of large external disturbances in the dynamic model. The controller is designed in three steps: Altitude control, position control (x and y motions), and attitude control (roll, pitch and yaw) as shown in Fig. 3.

In this section, a Fuzzy Sliding Mode Controller (FSMC) is designed; this controller combines the advantage of the SMC with FLS for the quadrotor aircraft robot. The SMC is designed to ensure the trajectory tracking and robustness against the internal and external disturbances. A FLS is designed to adapt the unknown switching-gains to reduce chattering phenomenon from fuzzifying the sliding surface according to the fuzzy inference rule base. The structure of the proposed controller-observer is shown in Fig. 3.

Motivated by practice, the measured UAV variables are linear position and yaw angle (x, y, z and ψ) and non-measurable states can be obtained by successive differentiation. However, they are contaminated by the measurement noise to a degree that the differentiation can no longer be used. For this reason, it is necessary to design an auxiliary dynamic system named observer, in this paper we have used an EKF as in Eq. (9), Eq. (10) and Eq. (11). The system input $u(t) = [u_1, u_2, u_3, u_4]^T$ and the measured response $Y = [x, y, z, \psi]^T$ are used by the observer EKF, where input u is applied to both quadrotor and extended Kalman filter. Desired vari-

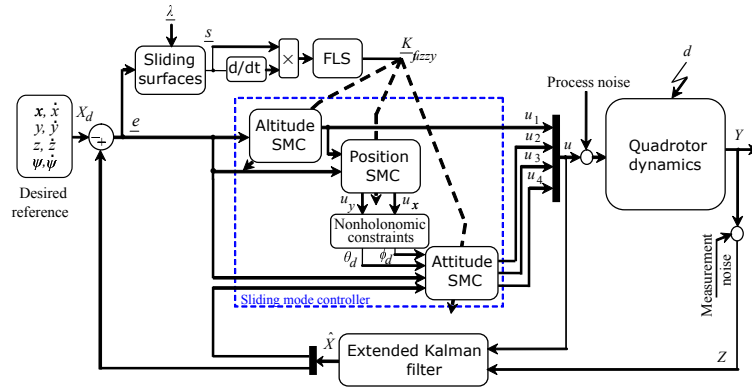


Fig. 3: Controller-observer system of the quadrotor robot.

ables and estimated velocity \hat{Y} of EKF are set to be inputs to the controller through a comparator. Note that the control will be impossible if the velocity cannot be measured.

5.1. Sliding Mode Control Design

If we define $\underline{e} = \hat{X} - X_d$ as the tracking error, the sliding surface \underline{s} is defined as [7]:

$$\underline{s} = \lambda \cdot \underline{e} + \dot{\underline{e}}, \tag{12}$$

where $\underline{s} = (s_1, s_2, \dots, s_6)^T$, $\dot{\underline{e}} = (\dot{e}_1, \dot{e}_2, \dots, \dot{e}_6)^T$ is the derivative vector of \underline{e} , $\lambda = \text{diag}(\lambda_1, \lambda_2, \dots, \lambda_6)$ with $\lambda_i > 0$.

Consider the derivative of the sliding surface defined as follows:

$$\dot{\underline{s}} = -\underline{K} \text{sgn}(\underline{s}) - \underline{\mu}(\underline{s}), \tag{13}$$

where $\underline{K} = \text{diag}(k_1, k_2, \dots, k_6)$, $k_i > 0$ are the switching-gains matrix entries to be tuned and $\underline{\mu} = \text{diag}(\mu_1, \mu_2, \dots, \mu_6)$, $\mu_i > 0$.

If the initial condition $\underline{e}(0) = 0$, the tracking problem $\hat{X} = X_d$ can be considered as the state error vector remaining on the sliding surface $\underline{s}(\underline{e}) = 0$. To achieve this condition, a Lyapunov function candidate is defined as:

$$V = \frac{1}{2} \underline{s}^T \underline{s}. \tag{14}$$

A sufficient condition for the stability of the system is given in [27] as follows:

$$\dot{V} = \frac{1}{2} \frac{d}{dt} \underline{s}^T \underline{s} \leq -\eta |\underline{s}|. \tag{15}$$

This leads to the following convergence condition:

$$\underline{s}^T \underline{s} \leq -\eta |\underline{s}| \Rightarrow \dot{\underline{s}} \cdot \text{sgn}(\underline{s}) \leq -\eta, \tag{16}$$

where $\eta > 0$, and $\text{sgn}(\cdot)$ denotes the signum function, it is defined as:

$$\text{sgn}(s_i) = \begin{cases} 1, & \text{if } s_i > 0, \\ 0, & \text{if } s_i = 0, \\ -1, & \text{if } s_i < 0. \end{cases}$$

Note that in Eq. (16): $|\underline{s}| = \frac{\underline{s}}{\text{sgn}(\underline{s})}$, by deriving Eq. (12):

$$\dot{\underline{s}} = \lambda \cdot \dot{\underline{e}} + \ddot{\underline{e}} = \lambda \cdot \dot{\underline{e}} + \ddot{X} - \ddot{X}_d. \tag{17}$$

Consider the control problem of the nonlinear system given in Eq. (5), replacing \ddot{X} with the state space equations, we get:

$$\dot{\underline{s}} = \underline{f}(X) + \underline{u}(X)u + d + \lambda \cdot \dot{\underline{e}} - \ddot{X}_d, \tag{18}$$

where $\underline{f} = (f_1, f_2, \dots, f_6)^T$ and $\underline{g} = (g_1, g_2, \dots, g_6)^T$.

Consider the EKF defined by Eq. (9), Eq. (10) and Eq. (11), by replacing X with \hat{X} , we get:

$$\dot{\underline{s}} = \underline{f}(\hat{X}) + \underline{g}(\hat{X})u + d + \lambda \cdot \dot{\underline{e}} - \ddot{X}_d. \tag{19}$$

From Eq. (13) and Eq. (19), and to satisfy the sliding condition Eq. (15), u^* has to be chosen so that \dot{V} is negative semi definite. Therefore, we can easily construct the SMC law:

$$u^* = u_{eq} + u_{dis} = \frac{1}{\underline{g}(\hat{X})} \cdot \left(-\underline{K} \text{sgn}(\underline{s}) - \underline{\mu} \cdot \underline{s} - \underline{f}(\hat{X}) - d - \lambda \cdot \dot{\underline{e}} + \ddot{X}_d \right), \tag{20}$$

where

$$\begin{aligned} u_{eq} &= \frac{1}{\underline{g}(\hat{X})} (-\underline{f}(\hat{X}) - d - \lambda \cdot \dot{\underline{e}} + \ddot{X}_d), \\ u_{dis} &= \frac{1}{\underline{g}(\hat{X})} (-\underline{K} \text{sgn}(\underline{s}) - \underline{\mu} \cdot \underline{s}). \end{aligned} \tag{21}$$

The equivalent control Eq. (21) is given by the following condition [27] $\underline{s} = 0$ and $\dot{\underline{s}} = 0 \Rightarrow u = u_{eq}$.

Based on assumptions 1–4 and considering that the estimate $\underline{g}(\hat{X})$ could be chosen according to the geometric mean $\underline{g}(\hat{X}) = \sqrt{g_{\max} \cdot g_{\min}}$, the bounds of $\underline{g}(X)$ may be expressed as $\beta^{-1} < \underline{g}(\hat{X})/g(X) < \beta$, where $\beta = \sqrt{g_{\max}/g_{\min}}$.

Under this condition, the switching-gains \underline{K} should be chosen according to:

$$\underline{K} \geq \beta(\eta + D + M) + (1 - \beta^{-1})|\hat{\tau}|, \quad (22)$$

where η is a strictly positive constant related to the reaching-time and $\hat{\tau} = -\underline{f}(\hat{X}) - d - \underline{\lambda}\dot{\underline{e}} + \ddot{X}_d$.

However, the use of discontinuous sgn function in the discontinuous control Eq. (20) will excite undesired phenomenon called chatter, which is caused by the inappropriate selection of the switching-gains matrix. In this context, high switching-gains matrix entries \underline{K} in Eq. (20) will increase the oscillations in the control signal, and therefore an excitation of high frequency dynamics will take place, as a result, a chattering phenomenon will be created. Moreover, a decrease in switching-gains can reduce the chattering phenomenon and improve the tracking performance despite noise and external disturbances. To achieve more appropriate performance, these switching-gains must be adjusted. This adjustment is based on the distance between the system states and the sliding surfaces. i.e., when the trajectory of the system states deviate from the sliding surfaces, the switching-gains should be increased in order to reduce chattering and vice versa. This idea can be realized by combining fuzzy logic with sliding mode control to construct FSMC to facilitate the adaptive switch-gains (see Fig. 3) according to some appropriate fuzzy rules. For this reason, one-input one-output FLS is designed in the next section.

5.2. Fuzzy Logic System

According to fuzzy logic systems [28], The fuzzy sets are defined as follows:

$$A_i = \{NB, NM, Z, PM, PB\},$$

$$B_i = \{NB, NM, Z, PM, PB\}.$$

Based on the experiences, the type of fuzzy rules is decided as “IF-THEN”.

The membership functions of input and output are chosen as illustrated in Fig. 4, in which the following linguistic variables have been used: Negative Big (NB), Negative Medium (NM), Zero (Z), Positive Medium (PM), and Positive Big (PB).

The fuzzy base rule of the adopted FLS contains five rules given in Tab. 1.

These rules govern the input-output relationship between \underline{s} and \underline{K}_{fuzzy} by adopting the Mamdani-type in-

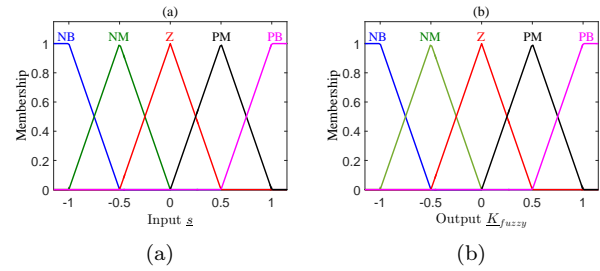


Fig. 4: (a) Input membership functions, (b) Output membership functions.

Tab. 1: Fuzzy rule set.

| | | | | | |
|-------------------------|----|----|---|----|----|
| \underline{s} | NB | NM | Z | PM | PB |
| \underline{K}_{fuzzy} | NB | NM | Z | PM | PB |

ference engine, in which the center of gravity method is used for defuzzification as in Eq. (23).

$$\underline{K}_{fuzzy} = \frac{\sum_{l=1}^N \zeta^l \left(\prod_{j=1}^n \mu_{A_j^l}(\underline{s}_j) \right)}{\sum_{l=1}^N \left(\prod_{j=1}^n \mu_{A_j^l}(\underline{s}_j) \right)}, \quad (23)$$

where N is the total number of fuzzy IF-THEN rules in the rule base, n is the number of system states. A_j^l and B_j^l denote fuzzy sets, ζ^l is the centre of gravity of the membership function of \underline{K}_{fuzzy} for the l^{th} rule. The Architecture of the FLS is shown in Fig. 5.

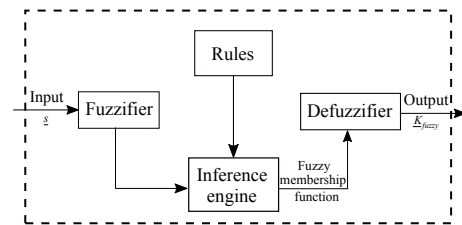


Fig. 5: The architecture of FLS.

Referring to Eq. (10), Eq. (11) and Eq. (13), the control law FSMC is now chosen as:

$$u = \frac{1}{\underline{g}(\hat{X})} \cdot \left(-\underline{K}_{fuzzy} \operatorname{sgn}(\underline{s}) - \underline{\mu}\underline{s} - \underline{f}(\hat{X}) - d - \underline{\lambda}\dot{\underline{e}} + \ddot{X}_d \right), \quad (24)$$

where $\underline{K}_{fuzzy} = \operatorname{diag}(\hat{k}_1, \hat{k}_2, \dots, \hat{k}_6)$, $\hat{k}_i > 0$ are the switching-gains matrix entries estimated by FLS. Note that the same FLS is used for all controllers (see Fig. 3).

5.3. Stability Analyses of the Proposed Controller-Observer

In order to demonstrate the stability of the closed-loop system, we adopt the following theorem:

Theorem 1. Consider the nonlinear system of Eq. (5) associated with the chosen sliding surfaces $\underline{s} = 0$. Under the assumptions 1–5, the estimation \hat{X} given by Eq. (9), (10), and (11), the switching-gains matrix \underline{K}_{fuzzy} adjusted by the FLS Eq. (19) and according to Eq. (22), therefore condition of Eq. (16) is satisfied and the tracking error will converge to zero asymptotically.

Proof. Proving the theorem above requires examining the sliding condition using the Lyapunov method.

Define the following positive definite Lyapunov function candidate $V = \frac{1}{2} \underline{s}^T \underline{s}$.

Its time derivative is given by:

$$\dot{V} = \frac{1}{2} \frac{d}{dt} \underline{s}^T \underline{s} = \underline{s}^T \dot{\underline{s}}. \quad (25)$$

Substituting Eq. (18) in Eq. (25) we get:

$$\dot{V} = \underline{s}^T (\underline{f}(X) + \underline{g}(X)u + d + \underline{\lambda} \cdot \dot{\underline{e}} - \ddot{X}_d). \quad (26)$$

Replacing the control u by Eq. (24), so that the derivative of the Lyapunov function becomes

$$\begin{aligned} \dot{V} &= \underline{s}^T \left[\underline{f}(X) + \underline{g}(X) \underline{g}^{-1}(\hat{X}) (-\underline{K}_{fuzzy} \text{sgn}(\underline{s}) + \underline{\mu} \cdot \underline{s} - \underline{f}(\hat{X}) - d - \underline{\lambda} \cdot \dot{\underline{e}} + \ddot{X}_d) + d + \underline{\lambda} \cdot \dot{\underline{e}} - \ddot{X}_d \right] = \\ &= \underline{s}^T \left[\underline{f}(X) + \underline{g}(X) \underline{g}^{-1}(\hat{X}) (-\underline{f}(\hat{X}) - d - \underline{\lambda} \cdot \dot{\underline{e}} + \ddot{X}_d) + \underline{g}(X) \underline{g}^{-1}(\hat{X}) (-\underline{K}_{fuzzy} \text{sgn}(\underline{s}) - \underline{\mu} \cdot \underline{s}) + d + \underline{\lambda} \cdot \dot{\underline{e}} - \ddot{X}_d \right]. \end{aligned}$$

Noting that: $\underline{f}(X) = \underline{f}(\hat{X}) - [\underline{f}(\hat{X}) - \underline{f}(X)]$, then

$$\begin{aligned} \dot{V} &= \underline{s}^T \left[\underline{f}(\hat{X}) - (\underline{f}(\hat{X}) - \underline{f}(X)) + \underline{g}(X) \underline{g}^{-1}(\hat{X}) \cdot \right. \\ &\cdot \left. (-\underline{f}(\hat{X}) - d - \underline{\lambda} \cdot \dot{\underline{e}} + \ddot{X}_d) + \underline{g}(X) \underline{g}^{-1}(\hat{X}) \cdot \right. \\ &\cdot \left. (-\underline{K}_{fuzzy} \text{sgn}(\underline{s}) - \underline{\mu} \cdot \underline{s}) + d + \underline{\lambda} \cdot \dot{\underline{e}} - \ddot{X}_d \right] = \\ &= \underline{s}^T \left[-(\underline{f}(\hat{X}) - \underline{f}(X)) + \underline{g}(X) \underline{g}^{-1}(\hat{X}) \hat{u} + \right. \\ &+ \underline{g}(X) \underline{g}^{-1}(\hat{X}) (-\underline{K}_{fuzzy} \text{sgn}(\underline{s}) - \underline{\mu} \cdot \underline{s}) - \hat{u} \left. \right] = \\ &= -\underline{s}^T \left[(\underline{f}(\hat{X}) - \underline{f}(X)) - \underline{g}(X) \underline{g}^{-1}(\hat{X}) \hat{u} + \right. \\ &+ \underline{g}(X) \underline{g}^{-1}(\hat{X}) (+\underline{K}_{fuzzy} \text{sgn}(\underline{s}) + \underline{\mu} \cdot \underline{s}) + \hat{u} \left. \right]. \end{aligned}$$

Therefore, considering Assumptions 2. and Assumptions 3., and defining \underline{K}_{fuzzy} according to Eq. (22), \dot{V} becomes $\dot{V} \leq -\eta |\underline{s}|$.

Dividing by $|\underline{s}|$ and integrating both sides over the interval $0 < t < t_s$ (t_s is the time required to reach \underline{s}),

gives:

$$\int_0^t \frac{\underline{s}}{|\underline{s}|} \dot{\underline{s}} d\tau \leq - \int_0^t \eta d\tau, \\ |\underline{s}(t = t_s)| - |\underline{s}(t = 0)| < -\eta t_s.$$

Considering t_{reach} as the time required to reach \underline{s} and noting that $|\underline{s}(t_{reach}) = 0|$, one has $t_{reach} \leq |\underline{s}(0)| / \eta$ and, consequently, the finite time convergence to the sliding surface \underline{s} . Thus, the tracking errors $X - X_d$ converge asymptotically to zero as $t \rightarrow +\infty$. \square

The synthesized control laws are given as follows:

1) Altitude Control

The altitude FSMC can be obtained by similar design procedures:

$$u_1 = \frac{m}{\cos x_1 \cos x_3} \left(-\hat{k}_6 \text{sgn}(s_z) + \right. \\ \left. -\mu_6 s_z - a_{11} x_{12} + g_a - \lambda_6 e_{12} + \ddot{z}_d - d \right), \quad (27)$$

where μ_6, λ_6 are positive real numbers.

From the dynamic Eq. (1), it can be seen that the motion through the axes x and y depends on u_1 . In fact, u_1 is the total thrust vector oriented to obtain the desired linear motion, by considering u_x and u_y are directing of u_1 responsible for the motion through x and y axes, respectively. Using FSMC, the control motion in the direction of x and y are obtained using the same steps described above.

$$\begin{aligned} u_x &= \frac{m}{u_1} \cdot \\ &\cdot \left(-\hat{k}_4 \text{sgn}(s_x) - \mu_4 s_x - a_9 x_8 - \lambda_4 e_8 + \ddot{x}_d - d \right), \\ u_y &= \frac{m}{u_1} \cdot \\ &\cdot \left(-\hat{k}_5 \text{sgn}(s_y) - \mu_5 s_y - a_{10} x_{10} - \lambda_5 e_{10} + \ddot{y}_d - d \right), \end{aligned}$$

where μ_i and λ_i , ($i = 4, 5$) are positive real numbers.

2) Attitude Control

Similar steps can be followed to design attitude FSMC laws for trajectory tracking control of roll, pitch, and yaw angles. The corresponding control laws are de-

signed as follows,

$$\begin{aligned}
 u_2 &= \frac{m}{b_1} \left(-\hat{k}_1 \operatorname{sgn}(s_\phi) - \mu_1 s_\phi - a_1 x_4 x_6 + \right. \\
 &\quad \left. - a_2 x_2^2 - a_3 \bar{\Omega} x_4 - \lambda_1 e_2 + \ddot{\phi}_d - d \right), \\
 u_3 &= \frac{m}{b_2} \left(-\hat{k}_2 \operatorname{sgn}(s_\theta) - \mu_2 s_\theta - a_4 x_2 x_6 + \right. \\
 &\quad \left. - a_5 x_4^2 - a_6 \bar{\Omega} x_2 - \lambda_2 e_4 + \ddot{\theta}_d - d \right), \\
 u_4 &= \frac{m}{b_3} \left(-\hat{k}_3 \operatorname{sgn}(s_\psi) - \mu_3 s_\psi - a_7 x_2 x_4 + \right. \\
 &\quad \left. - a_8 x_6^2 - \lambda_3 e_6 + \ddot{\psi}_d - d \right),
 \end{aligned}$$

where μ_i and λ_i , ($i = 1, 2, 3$) are positive real numbers.

The simplification of all computation steps concerning the tracking errors and sliding surfaces is defined as follows, respectively.

$$\begin{aligned}
 e : & \begin{cases} e_i = x_i - x_{id}, & i \in \{1, 3, 5, 7, 9, 11\}, \\ e_i = \dot{e}_{i-1}, & i \in \{2, 4, 6, 8, 10, 12\}, \end{cases} \\
 s : & \begin{cases} s_\phi = e_2 + \lambda_1 e_1 & s_x = e_8 + \lambda_4 e_7, \\ s_\theta = e_4 + \lambda_2 e_3 & s_y = e_{10} + \lambda_5 e_9, \\ s_\psi = e_6 + \lambda_3 e_5 & s_z = e_{12} + \lambda_6 e_{11}, \end{cases}
 \end{aligned}$$

6. Simulation and Discussions

In this section, the numerical simulation is conducted to demonstrate the performance of the controller-observer developed. In this simulation, the system's nominal parameters are shown in Tab. 2. The proposed controller-observer applied to the above quadrotor is simulated on a PC using MatLab environment (version 8.6.0.267246). A total of $N = 10000$ measurement data are simulated on a time interval from 0 to 10 seconds with step size $\Delta t = 0.001$ s. Note that the full program is coded in Matlab M-Files.

The initial condition for the quadrotor is $X(0) = 0_{12 \times 1}$, where $0_{12 \times 1}$ is a null vector, the controller parameters are selected as follows: $\mu = \operatorname{diag}(3, 3, 2, 2, 2, 4)$, $\lambda = \operatorname{diag}(10, 10, 3, 1, 1, 1)$. Two types of uncertainties are injected in the structure to verify the robustness of the controller-observer. The first one is an internal disturbance including the random Gaussian noise (process noise and measurement noise) both with covariance's $q = 10^{-2}$ and $r = 10^{-4}$, respectively, and with zero mean values. The second uncertainty is an external disturbance $\delta(t) = 0.01 \times \sin(2\pi t) \times I_{6 \times 1}$, where $I_{6 \times 1}$ is a vector, the upper bound of the disturbances is assumed to be $D = \max(|d|) = 1$. Note that these both disturbances sum up to $d(t)$ and they are applied at $t \geq 5$. EKF is implemented as in Eq. (9), Eq. (10) and Eq. (11) and will provide the state estimate vector $\hat{X} = [\hat{x}_1, \hat{x}_2, \dots, \hat{x}_{12}]^T$. The initial state and initial covariance conditions of the EKF are chosen to be $\hat{X}_{0/0} = 0_{12 \times 1}$ and $P_{0/0} = 1 \times I_{12 \times 12}$, respectively.

Note that the error covariance matrix P is set to be a 12×12 matrix, and covariance matrices Q and R are set to be 12×12 and 6×6 matrices, respectively, and they are experimentally set to:

$$\begin{aligned}
 Q &= \operatorname{diag}(q_{x_1}, \dots, q_{x_{12}}) = \\
 &= \begin{bmatrix} 10^{-2} & 0 & \dots & 0 \\ 0 & \ddots & \ddots & \vdots \\ \vdots & \ddots & \ddots & 0 \\ 0 & \dots & 0 & 10^{-2} \end{bmatrix},
 \end{aligned}$$

$$\begin{aligned}
 R &= \operatorname{diag}(r_{x_1}, r_{x_3}, r_{x_5}, r_{x_7}, r_{x_9}, r_{x_{11}}) = \\
 &= \begin{bmatrix} 10^{-1} & 0 & \dots & 0 \\ 0 & \ddots & \ddots & \vdots \\ \vdots & \ddots & \ddots & 0 \\ 0 & \dots & 0 & 10^{-1} \end{bmatrix},
 \end{aligned}$$

The Jacobean matrices F_k , W_k , H_k , and V_k for the Quadrotor are calculated as follows:

$$F_k = \begin{bmatrix} 1 & \Delta t & 0 & 0 & 0 & 0 & 0 & 0 & 0 & 0 & 0 & 0 \\ 0 & f_{22} & 0 & f_{24} & 0 & f_{26} & 0 & 0 & 0 & 0 & 0 & 0 \\ 0 & 0 & 1 & \Delta t & 0 & 0 & 0 & 0 & 0 & 0 & 0 & 0 \\ 0 & f_{42} & 0 & f_{44} & 0 & f_{46} & 0 & 0 & 0 & 0 & 0 & 0 \\ 0 & 0 & 0 & 0 & 1 & \Delta t & 0 & 0 & 0 & 0 & 0 & 0 \\ 0 & f_{62} & 0 & f_{64} & 0 & f_{66} & 0 & 0 & 0 & 0 & 0 & 0 \\ 0 & 0 & 0 & 0 & 0 & 0 & 1 & \Delta t & 0 & 0 & 0 & 0 \\ f_{81} & 0 & f_{83} & 0 & f_{85} & 0 & 0 & f_{88} & 0 & 0 & 0 & 0 \\ 0 & 0 & 0 & 0 & 0 & 0 & 0 & 0 & 1 & \Delta t & 0 & 0 \\ f_{10.1} & 0 & f_{10.3} & 0 & f_{10.5} & 0 & 0 & 0 & 0 & f_{10.10} & 0 & 0 \\ 0 & 0 & 0 & 0 & 0 & 0 & 0 & 0 & 0 & 0 & 1 & \Delta t \\ f_{12.1} & 0 & f_{12.3} & 0 & 0 & 0 & 0 & 0 & 0 & 0 & 0 & f_{12.12} \end{bmatrix},$$

$$H_k = \begin{bmatrix} 1 & 0 & 0 & 0 & 0 & 0 & 0 & 0 & 0 & 0 & 0 & 0 \\ 0 & 0 & 1 & 0 & 0 & 0 & 0 & 0 & 0 & 0 & 0 & 0 \\ 0 & 0 & 0 & 0 & 1 & 0 & 0 & 0 & 0 & 0 & 0 & 0 \\ 0 & 0 & 0 & 0 & 0 & 1 & 0 & 0 & 0 & 0 & 0 & 0 \\ 0 & 0 & 0 & 0 & 0 & 0 & 1 & 0 & 0 & 0 & 0 & 0 \\ 0 & 0 & 0 & 0 & 0 & 0 & 0 & 1 & 0 & 0 & 0 & 0 \end{bmatrix}, \tag{28}$$

$$W_k = I_{12 \times 12}, V_k = I_{6 \times 6},$$

where

$$\begin{aligned}
 f_{22} &= 2x_2 a_2 \Delta t + 1; & f_{24} &= \Delta t (x_6 a_1 + a_3 \bar{\Omega}); \\
 f_{26} &= x_4 a_1 \Delta t; & f_{42} &= \Delta t (x_6 a_4 + a_6 \bar{\Omega}); \\
 f_{44} &= 2x_4 a_5 \Delta t + 1; & f_{46} &= x_2 a_4 \Delta t; \\
 f_{62} &= x_4 a_7 \Delta t; f_{64} = x_2 a_7 \Delta t; & f_{66} &= 2x_6 a_8 \Delta t + 1; \\
 f_{81} &= \Delta t u_1 (C_1 S_5 - C_5 S_1 S_3) / m; \\
 f_{83} &= \Delta t u_1 (C_1 C_3 C_5 / m) / m; & f_{88} &= a_9 \Delta t + 1; \\
 f_{85} &= \Delta t u_1 (C_5 S_1 - C_1 S_3 S_5) / m; \\
 f_{10.1} &= -\Delta t u_1 (C_1 C_5 + S_1 S_3 S_5) / m; \\
 f_{10.3} &= \Delta t u_1 C_1 C_3 S_5 / m; & f_{10.10} &= a_{10} \Delta t + 1; \\
 f_{12.1} &= -\Delta t u_1 C_3 S_1 / m; & f_{12.3} &= -\Delta t u_1 C_3 S_1 / m; \\
 f_{12.12} &= a_{11} \Delta t + 1; \\
 C_i &= \cos(x_i), S_i = \sin(x_i), i = \{1, 3, 5\}.
 \end{aligned}$$

The desired trajectory components are chosen to be $x_d = 0.5 \cos(\pi/4t)$, $y_d = 0.5 \sin(\pi/4t)$, $z_d = 5$ and $\psi_d = 45^\circ$. The parameter values of the used quadrotor can be found in [1] and [2] and they can be seen at Tab. 2. The results obtained for the altitude and attitude tracking control of the quadrotor are given in the

Tab. 2: Quadrotor parameters.

| | | |
|--|-----------------------|--|
| $K_{fa} = \text{diag}(5.5670; 5.5670; 6.3540) \cdot 10^{-4} \text{ N}\cdot\text{rad}^{-1}\cdot\text{s}^{-1}$ | | |
| $K_{fd} = \text{diag}(0.032; 0.032; 0.048) \text{ N}\cdot\text{m}^{-1}\cdot\text{s}^{-1}$ | | |
| $J = \text{diag}(3.8278; 3.8278; 7.1345) \cdot 10^{-3} \text{ N}\cdot\text{m} \cdot \text{rad}^{-1}\cdot\text{s}^{-2}$ | | |
| $C_p = 2.9842 \cdot 10^{-5} \text{ N}\cdot\text{rad}^{-1}\cdot\text{s}^{-1}$ | | |
| $C_d = 3.2320 \cdot 10^{-7} \text{ N}\cdot\text{m} \cdot \text{rad}^{-1}\cdot\text{s}^{-1}$ | | |
| $J_r = 2.8385 \cdot 10^{-5} \text{ N}\cdot\text{m} \cdot \text{rad}^{-1}\cdot\text{s}^{-2}$, | | |
| $m = 400 \text{ g}$ | $l = 20.5 \text{ cm}$ | $g_a = 9.81 \text{ m}\cdot\text{s}^{-2}$ |
| $a_1 = -1$ | $a_2 = -0.1454$ | $a_3 = -0.0074$ |
| $a_4 = 1$ | $a_5 = -0.1454$ | $a_6 = 0.0074$ |
| $a_7 = -1.3061 \cdot 10^{-4}$ | | $a_8 = -0.0830$ |
| $a_9 = -0.0011$ | $a_{10} = -0.001$ | $a_{11} = -0.0013$ |
| $b_1 = 65.3117$ | $b_2 = 65.294$ | $b_3 = 130.6063$ |

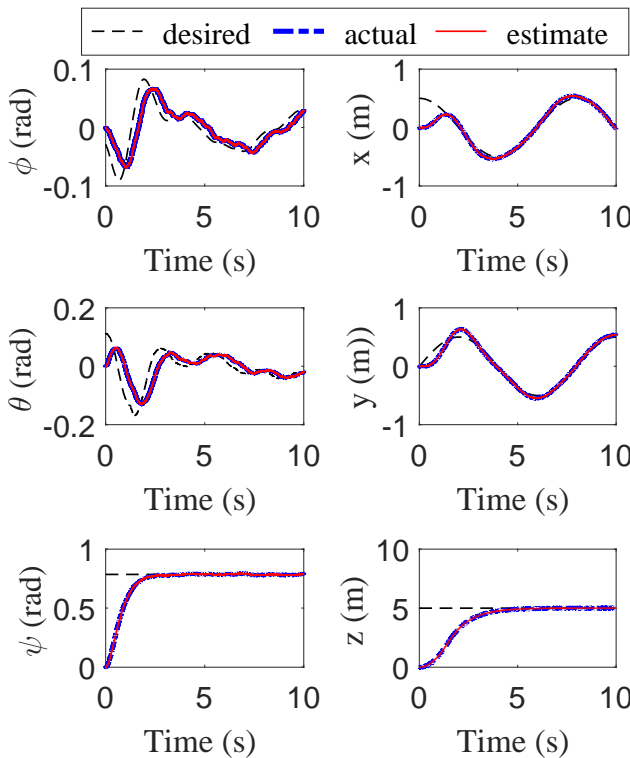


Fig. 6: Positions tracking.

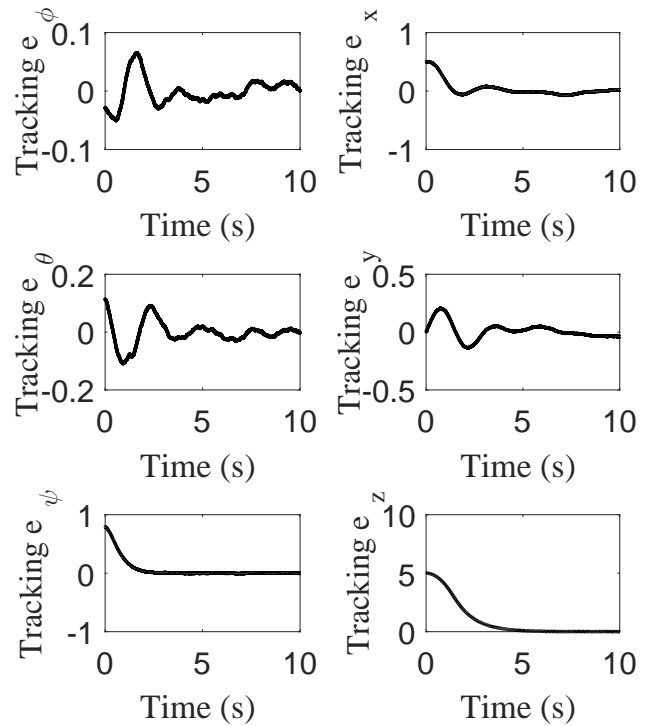


Fig. 7: Positions tracking errors.

Fig. 6, Fig. 7, Fig. 8, Fig. 9, Fig. 10, Fig. 11, Fig. 12 and Fig. 13.

Figure 6, Fig. 7, Fig. 8, Fig. 9, Fig. 10, Fig. 11, Fig. 12 and Fig. 13 show the simulation results obtained by the proposed method. Figure 6 and Fig. 7 show the output positions tracking and the positions tracking errors, respectively, where we observe that, the performances and robustness of the fuzzy sliding mode controller under the occurrence of internal and external disturbances are very acceptable. Figure 8 and Fig. 10 represent the velocities tracking, the velocities estimation errors, and the velocities tracking errors, respectively. It is clear that the estimated states converge to the desired ones (see Fig. 8), which shows a satisfactory estimation during the flight see Fig. 9. As it is clear from these figures, although we did not have measurements on velocities, EKF was able to es-

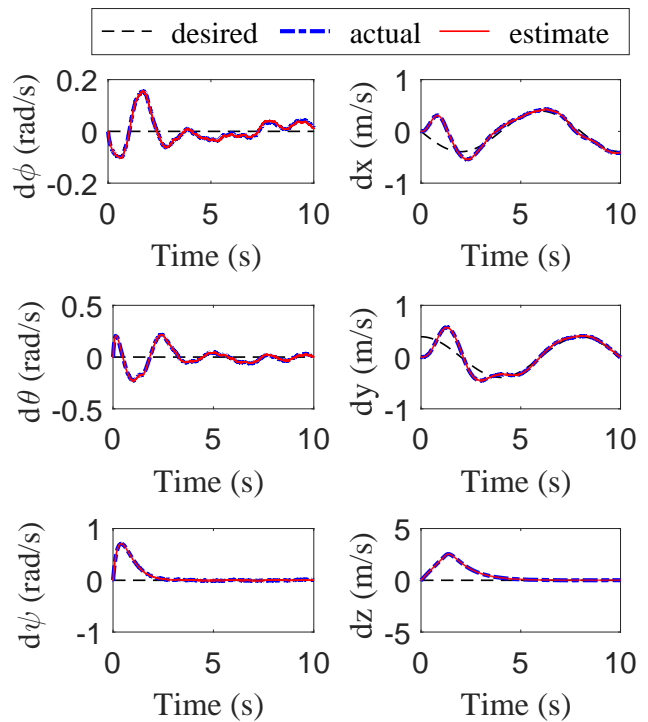


Fig. 8: Velocities tracking.

timate these values significantly. Figure 10 shows the velocities tracking errors, which all tend to zero after a finite time. The corresponding control inputs are depicted in Fig. 11, where we can clearly see that the chattering almost disappeared. It is noted that the discontinuities amplitudes are reduced. Compared

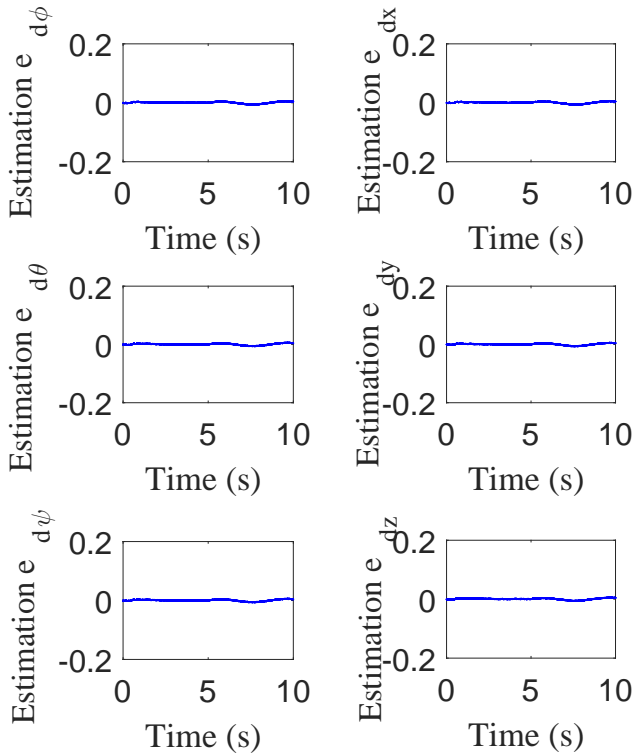


Fig. 9: Velocities estimation errors.

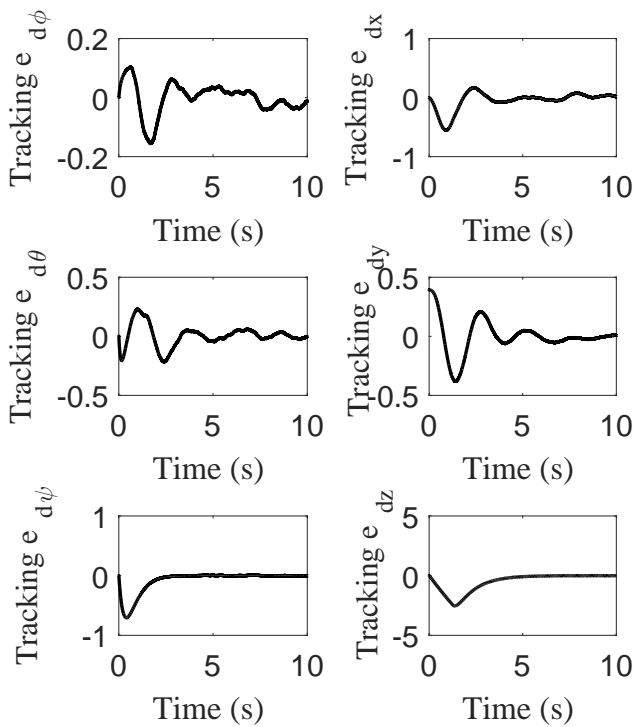


Fig. 10: Velocities tracking errors.

to the conventional SMC [8], we see clearly that the proposed control approach effectively reduces chattering phenomenon. The estimated fuzzy switching-gain curves are depicted in Fig. 12. We have also illustrated

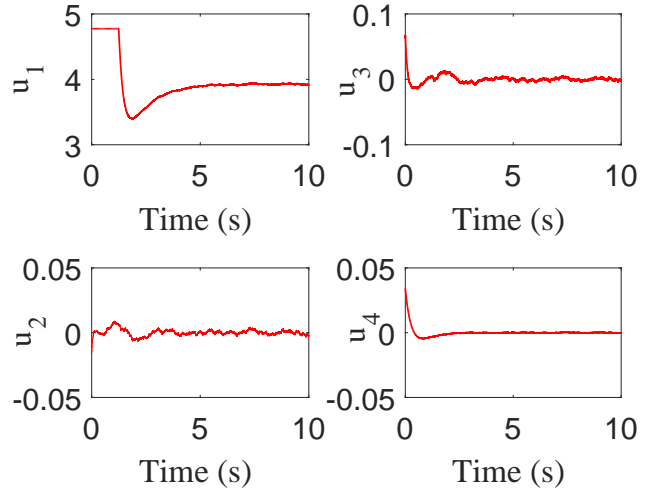


Fig. 11: Control inputs applied to quadrotor.

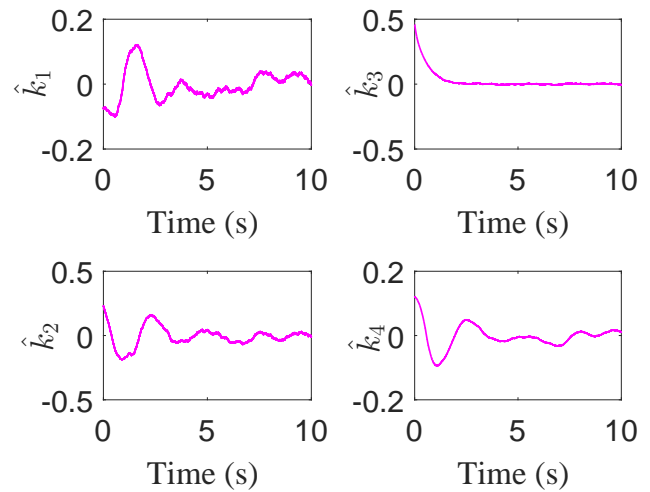


Fig. 12: Evolution of fuzzy switching-gains K_{fuzzy} .

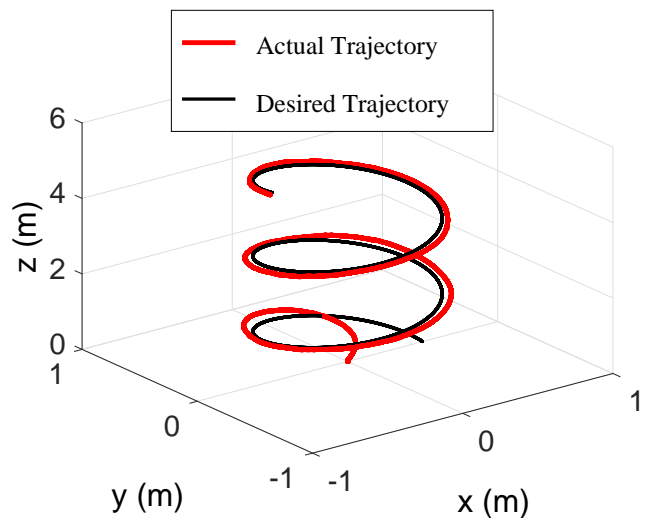


Fig. 13: Global tracking trajectory during 20s using: $x_d = 0.5 \cos(\pi/4t)$, $y_d = 0.5 \sin(\pi/4t)$, $z_d = 5t$, $\psi_d = 45^\circ$.

the global 3-D tracking trajectory of the quadrotor in Fig. 13.

7. Conclusion

In this paper, we presented an EKF based states estimation, and altitude-attitude tracking control for unmanned quadrotor despite the presence of internal and external disturbances. We assumed that not all states are measured; therefore an EKF system to estimate the hidden states in order to avoid hardware sensors was introduced. Sliding mode control was applied, and it was enhanced by a fuzzy system to adapt the unknown switching-gains in order to eliminate the chattering phenomenon. Based on the simulation results, we conclude that the proposed controller-observer performs well. This reflect the robustness and performances of the mixed controller-observer, which was also confirmed by the tracking an estimation errors convergence. The stability of the proposed approach was guaranteed by Lyapunov stability criterion. Simulation results confirmed the ability of proposed controller-observer to ensure a good estimation and yield superior control performances for nonlinear system control against internal and external disturbance simultaneously.

References

- [1] CASTILLO, P., A. DZUL and R. LOZANO. Real-time stabilization and tracking of a four-rotor mini rotorcraft. *IEEE Transactions on Control Systems Technology*. 2004, vol. 12, iss. 4, pp. 510–516. ISSN 1558-0865. DOI: 10.1109/TCST.2004.825052.
- [2] DERAFA, L., T. MADANI and A. BENALLEGUE. Dynamic Modelling and Experimental Identification of Four Rotors Helicopter Parameters. In: *2006 IEEE International Conference on Industrial Technology*. Mumbai: IEEE, 2006, pp. 1834–1839. ISBN 1-4244-0725-7. DOI: 10.1109/ICIT.2006.372515.
- [3] XIONG, J.-J. and E.-H. ZHENG. Position and attitude tracking control for a quadrotor UAV. *ISA Transactions*. 2014, vol. 53, iss. 3, pp. 725–731. ISSN 0019-0578. DOI: 10.1016/j.isatra.2014.01.004.
- [4] TAYEBI, A. and S. MCGILVRAY. Attitude stabilization of a VTOL quadrotor aircraft. *IEEE Transactions on Control Systems Technology*. 2006, vol. 14, iss. 3, pp. 562–571. ISSN 1558-0865. DOI: 10.1109/TCST.2006.872519.
- [5] ZUO, Z. Trajectory tracking control design with command-filtered compensation for a quadrotor. *IET Control Theory & Applications*. 2010, vol. 4, iss. 11, pp. 2343–2355. ISSN 1751-8652. DOI: 10.1049/iet-cta.2009.0336.
- [6] LIMNAIOS, G. and N. TSOURVELOUDIS. Fuzzy Logic Controller for a Mini Coaxial Indoor Helicopter. *Journal of Intelligent & Robotic Systems*. 2012, vol. 65, iss. 1–4, pp. 187–201. ISSN 1573-040. DOI: 10.1007/s10846-011-9573.
- [7] SLOTINE, J.-J. Sliding controller design for nonlinear systems. *International Journal of Control*. 1983, vol. 40, iss. 2, pp. 421–434. ISSN 0020-7179. DOI: 10.1080/00207178408933284.
- [8] ZEGHLACHE, S., D. SAIGAA, K. KARA, A. HARRAG and A. BOUGUERRA. Fuzzy Based Sliding Mode Control Strategy For An Uav Type-quadrotor. *Mediterranean Journal of Measurement and Control*. 2012, vol. 8, iss. 3, pp. 436–446. ISSN 1743-9310.
- [9] MOKHTARI, A., A. BENALLEGUE and Y. ORLOV. Exact linearization and sliding-mode observer for a quadrotor unmanned aerial vehicle. *International Journal of Robotics and Automation*. 2006, vol. 21, iss. 1, pp. 39–49. ISSN 0826-8185. DOI: 10.2316/Journal.206.2006.1.206-2842.
- [10] BENALLEGUE, A., A. MOKHTARI and L. FRIDMAN. High order sliding-mode observer for a quadrotor UAV. *International Journal of Robust and Nonlinear Control*. 2007, vol. 18, iss. 4–5, pp. 427–440. ISSN 1099-1239. DOI: 10.1002/rnc.1225.
- [11] MEDJGHOU, A., M. GHANAI and K. CHAFAA. BBO optimization of an EKF for interval type-2 fuzzy sliding mode control. *International Journal of Computational Intelligence Systems*. 2015, vol. 19, iss. 4, pp. 851–858. ISSN 1433-7479. DOI: 10.2991/ijcis.11.1.59.
- [12] KANG, H.-S., Y. LEE, C.-H. HYUN, H. LEE and M. PARK. Design of sliding-mode control based on fuzzy disturbance observer for minimization of switching gain and chattering. *Soft Computing*. 2018, vol. 11, iss. 1, pp. 770–789. ISSN 1875-6883.
- [13] DIERKS, T. and S. JAGANNATHAN. Output Feedback Control of a Quadrotor UAV Using Neural Networks. *IEEE Transactions on Neural Networks*. 2010, vol. 21, iss. 1, pp. 50–66. ISSN 1941-0093. DOI: 10.1109/TNN.2009.2034145.
- [14] BOUTAYEB, M., H. RAFARALAHY and M. DAROUACH. Convergence analysis of the extended Kalman filter used as an observer for nonlinear deterministic discrete-time systems. *IEEE Transactions on Automatic Control*. 1997, vol. 42, iss. 4, pp. 581–586. ISSN 1558-2523. DOI: 10.1109/9.566674.

- [15] MANES, C., F. PARASILITI and M. TURSIN. A comparative study of rotor flux estimation in induction motors with a nonlinear observer and the extended Kalman filter. In: *Proceedings of IECON'94 - 20th Annual Conference of IEEE Industrial Electronics*. Bologna: IEEE, 1994, pp. 2149–2154. ISBN 0-7803-1328-3. DOI: 10.1109/IECON.1994.398152.
- [16] XU, Z. and M. F. Rahman. Comparison of a Sliding Observer and a Kalman Filter for Direct-Torque-Controlled IPM Synchronous Motor Drives. *IEEE Transactions on Industrial Electronics*. 2012, vol. 59, iss. 11, pp. 4179–4188. ISSN 1557-9948. DOI: 10.1109/TIE.2012.2188252.
- [17] CHEN, Z. *Sensorless Control of Permanent Magnet Synchronous Machines With Multiple Saliencies*. Munich, 2015. Dissertation thesis. Technical University of Munich. Supervisor: Prof. Dr. Ing. Wolfgang Kellerer.
- [18] MEDJGHOUE, A., M. GHANAI and K. KHEIREDDINE. A Robust Feedback Linearization Control Framework Using an Optimized Extended Kalman Filter. *Journal of Engineering Science & Technology Review*. 2017, vol. 10, iss. 5, pp. 1–16. ISSN 1791-2377. DOI: 10.25103/jestr.105.01.
- [19] MEDJGHOUE, A., M. GHANAI and K. CHAFAA. Improved Feedback Linearization Control Based on PSO Optimization of an Extended Kalman Filter. *Optimal Control Applications and Methods*. 2018, vol. 39, iss. 6, pp. 1–16. ISSN 1099-1514. DOI: 10.1002/oca.2454.
- [20] ZEGHLACHE, S., D. SAIGAA, K. KARA and A. BOUGUERRA. State vector estimation using extended filter kalman for the sliding mode controlled quadrotor helicopter in vertical flight. In: *2013 8th International Conference on Electrical and Electronics Engineering (ELECO)*. Bursa: IEEE, 2013, pp. 492–496. ISBN 978-605-01-0504-9. DOI: 10.1109/ELECO.2013.6713891.
- [21] BENZERROUK, H., A. NEBYLOV and H. SALHI. Quadrotor UAV state estimation based on High-Degree Cubature Kalman filter. *IFAC-PapersOnLine*. 2016, vol. 49, iss. 17, pp. 349–354. ISSN 2405-8963. DOI: 10.1016/j.ifacol.2016.09.060.
- [22] LI, S., Y. WANG, J. TAN and Y. ZHENG. Adaptive RBFNNs/integral sliding mode control for a quadrotor aircraft. *IFAC-PapersOnLine*. 2016, vol. 54, iss. 1, pp. 208–217. ISSN 0925-2312. DOI: 10.1016/j.neucom.2016.07.033.
- [23] YANG, Y. and Y. YAN. Attitude regulation for unmanned quadrotors using adaptive fuzzy gain-scheduling sliding mode control. *Aerospace Science and Technology*. 2016, vol. 216, iss. 1, pp. 126–134. ISSN 1270-9638. DOI: 10.1016/j.ast.2016.04.005.
- [24] REINOSO, M., L. I. MINCHALA, P. ORTIZ, D. F. ASTUDILLO and D. VERDUGO. Trajectory tracking of a quadrotor using sliding mode control. *IEEE Latin America Transactions*. 2016, vol. 14, iss. 5, pp. 2157–2166. ISSN 1548-0992. DOI: 10.1109/TLA.2016.7530409.
- [25] MEDJGHOUE, A., N. SLIMANE and K. CHAFAA. Fuzzy sliding mode control based on backstepping synthesis for unmanned quadrotors. *Advances in Electrical and Electronic Engineering*. 2018, vol. 16, no. 2, pp. 135–146. ISSN 0021-9223. DOI: 10.15598/aeec.v16i2.2231.
- [26] KALMAN, R. E. A new approach to linear filtering and prediction problems. *Journal of Basic Engineering*. 1960, vol. 82, iss. 1, pp. 35–45. ISSN 1804-3119. DOI: 10.1115/1.3662552.
- [27] SLOTINE, J.-J. E. and W. LI. *Applied Nonlinear Control*. 1st ed. London: Prentice-Hall, Inc., 1991. ISBN 01-304-0890-5.
- [28] WANG, L.-X. Stable adaptive fuzzy control of nonlinear system. *IEEE Transactions on Fuzzy Systems*. 1993, vol. 1, iss. 2, pp. 146–155. ISSN 1941-0034. DOI: 10.1109/91.227383.

About Authors

Mouna GHANAI was born in Batna, Algeria, in 1975. She received the Engineer degree in Industrial Control from Batna University, Algeria, in 1999, Master degree in Industrial Control from Setif University, Algeria, in 2006 and the Doctorate Es-Science grade in electronic from Batna University, Algeria, in 2013. Currently, she is an Assistant Professor with the department of Electronics, Faculty of Technology, University Batna 2 Mostefa BenBoulaïd, Batna, Algeria. His research interests include modelling and identification of nonlinear systems, automatic control, and biomedical signal processing

Ali MEDJGHOUE He received the Bachelor degree in Automatic, Master degree in Advanced Automatic from Electrical Engineering Department, University of Biskra, Algeria, in 2010 and 2012, respectively. He received his Doctorate degree in robotics and artificial intelligence from Electronics Department, University of Batna 2 Mostefa

BenBoulaid, Batna, Algeria, in 2018. He is attached of research to (LAAAS) laboratory, University of Batna 2 Mostefa BenBoulaid, Algeria. His research interests include dynamics, robotics, systems and controls, optimization, soft computing, and simulation.

Kheireddine CHAFAA was born in Batna, Algeria, in 1971. He received the Engineer, Magister

and Doctorate Es-Science diplomas in Industrial Control from Batna University, Algeria, in 1994, 1999, and 2006 respectively. Currently, he is a Professor with the department of Electronics, Faculty of Technology, University Mostefa BenBoulaid, Batna 2, Algeria. Her research interests include modeling and identification of nonlinear systems, nonlinear and adaptive control, soft computing, and biomedical signal processing.